Metallomics

Accepted Manuscript

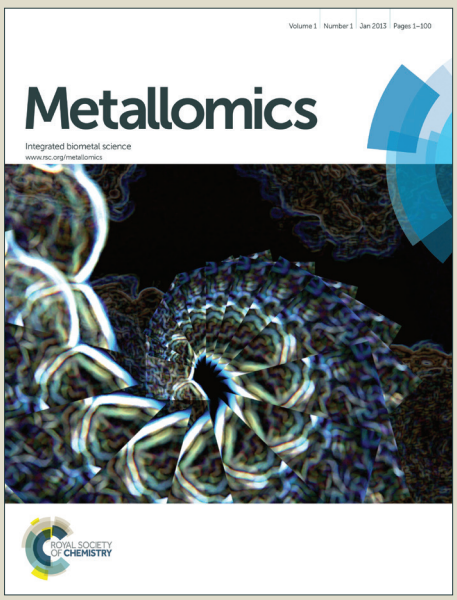

ROYAL SOCIETY OF CHEMISTRY

www.rsc.org/metallomics

Correlations in Distribution and Concentration of Calcium, Copper and Iron with Zinc in Isolated Extracellular Deposits Associated with Age-Related Macular Degeneration

Jane M. Flinn[1], Peter Kakalec[1], Ryan Tappero[2], Blair Jones[3] and Imre Lengyel[4*]

[1]Psychology, George Mason University, Fairfax, VA, USA

[2]National Synchrotron Light Source, Brookhaven National Laboratory, Upton, NY, USA

[3]US Geological Survey, Reston, VA, USA

[4]UCL Institute of Ophthalmology, University College London, London, UK

*To whom correspondence should be addressed:
Imre Lengyel PhD
UCL Institute of Ophthalmology
University College London
11-43 Bath Street, London,
EC1V 9EL
United Kingdom
e-mail: i.lengyel@ucl.ac.uk
Tel: +44 (0)20 7608 6894
Fax: +44 (0)20 7608 6862

Abstract

Zinc (Zn) is abundantly enriched in sub-retinal pigment epithelial (RPE) deposits, the hallmarks of age-related macular degeneration (AMD), and is thought to play a role in the formation of these deposits. However, it is not known whether Zn is the only metal relevant for sub-RPE deposit formation. Because of their involvement in the pathogenesis of AMD, we determined the concentration and distribution of calcium (Ca), iron (Fe) and copper (Cu) and compared these with Zn in isolated and sectioned macular (MSD), equatorial (PHD) and far peripheral (FPD) sub-RPE deposits from an 86 year old donor eye with post mortem diagnosis of early AMD. The sections were mounted on Zn free microscopy slides and analyzed by microprobe synchrotron X-ray fluorescence (μSXRF). Metal concentrations were determined using spiked sectioned sheep brain matrix standards, prepared the same way as the samples. The heterogeneity of metal distributions was examined using pixel by pixel comparison. The orders of metal concentrations were Ca>>>Zn>Fe in all three types of deposits but Cu levels were not distinguishable from background values. Zinc and Ca were consistently present in all deposits but reached highest concentration in MSD. Iron was present in some but not all deposits and was especially enriched in FPD. Correlation analysis indicated considerable variation in metal distribution within and between sub-RPE deposits. The results suggest that Zn and Ca are the most likely contributors to deposit formation especially in MSD, the characteristic risk factor for the development of AMD in the human eye.

Keywords: zinc; calcium, iron, copper, drusen; sub-RPE deposit; Bruch's membrane; retina; age-related macular degeneration; metals

Introduction

Many neurodegenerative disorders of the central nervous system are characterized by extracellular protein aggregation and deposition, often mediated by metals such as zinc (Zn), calcium (Ca), iron (Fe) and copper (Cu) [1-4]. In age-related macular degeneration (AMD), the major cause of blindness in the developed world [5], extracellular deposits are formed in the so-called Bruch's membrane, a penta-laminal extracellular matrix interposed between the retinal pigment epithelium (RPE) and the choroidal vasculature. These sub-RPE deposits can be focal (recognized clinically as drusen) or diffuse (basal laminar or linear deposits, depending on whether they are present internal or external of the RPE basement membrane) [5]. The composition of sub-RPE deposits had been studied most extensively at the macula [6-8], the site of central vision, as drusen are integral to the pathogenesis of AMD [5]. Sub-RPE deposit formation also occurs at the retinal periphery [9] and there are indications that pathological events at the retinal periphery are important in understanding degenerative diseases such as AMD [10-13]. Proteins and lipids are abundantly present in sub-RPE deposit and the high concentration of Zn found in these deposits suggested that Zn was directly involved in deposit formation through the oligomerization of proteins [1, 14-18]. However, the pathological events leading to AMD had also been associated with Ca, Fe and Cu [7, 19-23], but the concentration and distribution of these metals in sub-RPE deposit was not known. Here we determined, for the first time, the concentration and distribution of Ca, Fe and Cu and correlated these with Zn in isolated sub-RPE deposits isolated from three geographic locations from a human eye with early AMD.

Materials and Methods

Tissue Preparation

After examining a number of cadaveric human eyes, only the eyes of an 86 year old donor contained significant deposits in the macula, equator and far periphery simultaneously (Fig 1, A), which allowed for direct comparison of the metals in these three geographic locations. Tissues for this project were obtained from the UCL Institute of Ophthalmology and Moorfields Eye Hospital Eye Tissue Repository within 24 hours of death. Full Local Research Ethics Committee approval and appropriate consent were obtained in all cases. The protocol of our study adhered to the tenets of the Declaration for Helsinki regarding research involving human tissue.

Preparation of the tissues was exactly as described previously [9, 24]. In short, a circular cut were made on the sclera at the *ora serrata* to remove the front of the eye. To flat mount the back of the eye, containing the neurosensory retina, retinal pigment epithelium and the choroid, incisions were made from the *ora serrata* towards to the optic nerve head. The first and longest incision determined the direction of the optic nerve head and the pigment rich fovea. Following the removal of the vitreous body and the neurosensory retina, the RPE cells were removed by gentle agitation. The Bruch's membrane/choroid complex was cut around the optic nerve head and then gently removed from the sclera. Further incisions were made to render the quasi-spherical retina into a 2D preparation. The shape of a typical flat mount can be seen on Fig 1A. Flat mounts were imaged using a Nikon SMZ 1500 fluorescence binocular microscope first under bright field than by using tissue autofluorescence in blue light [9]. Visualization of sub-RPE deposits was enhanced by labeling the deposits with ZinPyr1 (NeuroBiotex, Galveston, USA), the Zn selective fluorescent sensor [24]. Image series' were stitched together using Panotur Pro 1.8 (Kolor SARL). This labeling allowed a more precise post-mortem phenotyping that identified large sub-RPE deposits in the macula (macular soft

drusen=MSD), equator (peripheral hard drusen=PHD), and the far periphery (far peripheral deposit=FPD), which were isolated as described earlier [6]. Isolated samples were embedded in optimal cutting temperature (OCT) compound, frozen in acetone/dry ice slurry and sectioned using a cryostat 20 µm. Using the adaptation of a recently developed algorithm "Retistruct" [25] we reconstructed retinal flat-mounts by mapping them into a standard, spherical retinal space (Fig 1 C and D).

Microprobe synchrotron X-ray fluorescence

Microprobe synchrotron X-ray fluorescence (µSXRF), a non-destructive technique which measures the total metal abundance in a sample, was performed at Beamline X27A, National Synchrotron Light Source, Brookhaven National Laboratory. The incident X-ray beam was tuned to 10 keV using a Si(111) channel-cut monochromator. This monochromatic beam is focused to 10 µm in diameter using Rh-coated silicon microfocusing mirrors in Kirkpatrick-Baez type geometry. Energy dispersive X-ray fluorescence data were collected using a Canberra 13-metal Ge Array detector. This method can be used to measure the metal concentrations at one place, or to determine the average concentration across an area. Metal concentrations can be determined in different samples with detection limits as low as 0.1-5 ppm [26, 27].

To determine metal distributions and co-localizations throughout the flat mount whole retina, a 0.4 mm X 25 mm long strip was dissected and placed on a Zn-free slide (Heraeus) and sampled at 200 µm steps with a 10 µm wide X-ray beam to obtain µSXRF images for Ca, Zn, Cu and Fe (Fig 1, B). To determine metal concentrations in sub-RPE deposits (Fig 2), twenty micron thick OCT embedded sections were placed on Zn-free slides (Heraeus) and analyzed by µSXRF metal using 10 µm steps with a 7 sec integration time. For quantitative evaluations, brain-matrix standards were made from cryostat-prepared sections (20 µm) of homogenized fresh sheep isocortex spiked with, 10, 25, 50, 100 and 250 PPM of Zn, Ca, Fe,

and copper. Higher concentrations could not be used as this led to tissue inhomogeneity. Emission values from the sheep brain standards were used for calculation of metal concentration in the sub-RPE deposits in ppm.

Results and Discussion

The eye from the 86 year-old donor showed deposits in the macula, equator and far periphery simultaneously (Fig. 1A). A 0.4 mm X 25 mm strip was scanned first using μSXRF to analyze the general distribution of Ca, Zn, Cu and Fe from the macula to the *ora serrata*. The false color plots of the emission intensities expressed as counts per second (CPS) values are seen on Fig.1B. These show that all four metals are present throughout this tissue but their distributions differ depending on geographic location (Fig 1B). When metal contents were correlated pixel by pixel to examine co-localization, we found significant correlation between Zn and Ca (R: 0.676; $p < 0.01$), but no significant correlations could be observed between other metal combinations. Given the large step size (200 μm) and small beam diameter (10 μm), this measurement was not intended to determine metal distribution in individual deposits but to gain an overview of the metal distribution and co-localization in the Bruch's membrane choroid complex. Occasionally, especially in the case of large FPD, the sampling inevitably included sub-RPE deposits. This analysis did not reproduce the correlation between Zn and Cu in the Bruch's membrane choroid complex reported earlier [23, 28], probably due to the fact that we only sampled one donor eye.

To determine Zn, Ca, Fe and Cu concentration and distribution in isolated sub-RPE deposits, soft drusen (>125 μm) in the macula (on Fig. 1A these are labeled MSD), hard drusen (<63 μm) at the periphery (labeled PHD) and large (>200 μm) sub-RPE deposits at the far periphery (labeled FPD) were isolated manually from the Bruch's membrane, embedded and then sectioned in OCT at 20 μm. The metal distributions were determined by μSXRF (Fig. 2). Optical images of the sections from sub-RPE deposits are shown on Fig 2 A, F and K. The false color images are scaled to the maximum CPS values for individual metals, giving visual information on co-localization. To identify the relationship between concentrations, the CPS values were converted to concentration in parts per million (PPM).

For this we used standard curves generated from spiked sheep brain matrix as described earlier [24]. Zinc concentrations in MSD were higher than those in PHD or FPD (Table 1). These Zn concentrations show good agreement with those reported earlier using the same detection method, but from other donors [24], building confidence in our approach using isolated deposits.

Calcium concentrations appeared very high in all three types of deposits, with the highest concentrations measured in MSD, with ~30 times less in FPD and a further 10 times less in PHD (Table 1). Whether the unexpectedly high Ca concentrations (Table 1) reflect exact values or arise from interpolation from the limited maximum concentration used to generate the standard curves (250 PPM) will need to be investigated further. However, our data clearly show that Ca is present in very high concentration in all sub-RPE deposits. The presence, but not the concentration, of Ca in sub-RPE deposits had been shown as early as 1987 by using classic freeze-fracture and scanning electron microscope based elemental analysis [29]. Alongside Ca, phosphate was also detected in sub-RPE deposits suggesting that Ca might be present in a Ca-phosphate complex which gained further supported after labeling of deposits by von Kossa staining [19]. Crystalline Ca-phosphate does contain high weight percent Ca [30] which may explain the high PPM values in our measurements.

Iron concentrations differed only slightly between the different eccentricities though FPD appear to contain the highest concentration of this metal (Table 1). It is important to note that not all deposits contained Fe. Fe had been associated with AMD [31], but its concentration in sub-RPE deposits had not been determined before.

By analyzing the false color images it was apparent that Cu was not enriched in sub-RPE deposits (Fig. 2), suggesting that if it was present, than its concentration was below the detection limit. As changes in Cu levels in the RPE choroid complex had been shown to be

associated with AMD [23, 28] this association appears to be locate Cu outside the sub-RPE deposits.

When metal concentrations were correlated with each other pixel by pixel we found large variability in co-distributions (Fig. 3). The best correlations were observed in the FPD between Zn and Ca, followed by Zn and Fe, but correlations between other metal combinations and different eccentricities produced low R values (Table 2) indicating that different metals are mainly located in separate micro-compartments.

Conclusions

Knowledge of the molecular composition of sub-RPE deposits, the hallmarks of AMD, in the outer retina is thought to be essential to develop new intervention strategies for preventing the development or slowing the progression of AMD. Sub-RPE deposits contain a large number of different proteins [6, 32-38], lipids and lipid by-products [39-43] as well as metals [20, 22, 24, 31, 44]. Previously we determined the concentrations of Zn in macular and peripheral sub-RPE deposists [24], but the concentration of metals like Ca, Fe and Cu and their co-distribution with zinc was not known. Here we report, for the first time, how Zn concentration and distribution is associated with those of Ca, Fe and Cu in isolated sub-RPE deposits from three different geographic locations of the retina from a cadaveric human eye with MSD, the hallmark of early of AMD.

Zinc, Ca, Fe and Cu are important for normal function in the intracellular as well as in the extracellular environment around the RPE and the choroid, such that more complete knowledge of the control of their levels and distribution might hold the key to better treatment in AMD. By analogy with Alzheimer's disease, buffering the bio-available Zn (and probably Cu and Fe), in the extracellular fluids of the brain lead to a striking dissolution and clearance of amyloid plaques [1] and favorable changes in disease progression [2, 4]. The possibility that similar approaches may interdict sub-RPE deposit formation is intriguing.

There are many proteins identified in sub-RPE deposits that bind metals for their normal function [6]. However, based on the very high concentrations of Ca and Zn we found in sub-RPE deposits, the most likely scenario is that these metal concentrations will induce pathological protein-metal interactions such as the metal-amyloid beta-interactions [1, 2, 45] and the interactions between components of the complement cascade and metals [14-18]. The high concentrations of Zn in sub-RPE deposits could certainly trigger the oligomerization of these, and probably other, proteins and contribute to the buildup of the pathological protein rich

deposits. It is interesting to note that oligomerization of complement factor H (CFH) was also induced by Cu, but not Ca or Fe *in vitro* [17]. Given the absence of Cu in isolated sub-RPE deposits, the most likely mediator of CFH oligomarization *in vivo* is Zn.

Sub-RPE deposits are heterogeneous in their internal structure [9, 24, 32, 46] and protein composition [6], therefore it is perhaps not surprising that there is high degree of inhomogeneity in metal distributions in them. The high degree of heterogeneity from a single donor indicates that metal inhomogeneity might be an inherent feature of sub-RPE deposits and preliminary data on sub-RPE deposits still attached to the Bruch's membrane/choroid complex in several donor eyes appears to support this (Flinn and Lengyel, unpublished information).

While it will be important to undertake similar studies on isolated sub-RPE deposits from eyes of other donors and from a varied ethnic background, our data from a single donor yielded very valuable information. The most intriguing finding of this study was the unusually high concentration of Ca in all examined sub-RPE deposits. We did expect to find Ca in sub-RPE deposits, as calcification had been reported in relation to aging and AMD [19, 44]. However, based on the qualitative assessments we did not expect to find Ca concentrations up to 10^6 PPM. The biological significance of such high Ca accumulation in sub-RPE deposits is not yet known, but it might be relevant to understand how deposits in general and the so-called calcified drusen specifically develop [47].

Clearly metal accumulations in sub-RPE deposit can be bad for AMD, due to their potential involvement at the initial step on the way to blindness. However, metals can also be good for AMD at the late stages of the disease by slowing the progression to blindness in choroidal neovascularization , evidence by studies using zinc supplementation [48]. Therefore, whether Zn is good or bad will likely depend on at which stage(s) of AMD they are involved in [49]. Based on analogy to Zn, it might be important to examine how homeostatic or supplementary changes in other metals might influence the different stages of AMD.

We are at the early stages of understanding how sub-RPE deposits are formed and the factors that influence this process. The role of metals in the pathogenesis of AMD is likely to be complex since they can bind to a multitude of proteins and peptides and interact or compete with each other in many biochemical processes. It is becoming evident that AMD comprises a wide spectrum of diseases and that decision on treatment strategies will depend on many factors that may include the better understanding how Zn, Ca, Fe and Cu alone or in combination contribute to the progression of this blinding disease. The fact that we presented evidences for high concentrations of Zn and Ca especially in the macular soft drusen suggests that understanding their origin, mechanisms of action and regulation of availability at the Bruch's membrane/choroid complex could lead to new intervention strategies that delay sub-RPE deposit formation and, as a consequence, slow the onset of AMD.

Acknowledgements: We thank Professors Alan C Bird, Richard Thompson and Erinn Gideon for their generous help and Dr David Sterratt for reconstructing the flat mounted samples. The research was supported by the Bill Brown Charitable Trust Senior Research Fellowship, Moorfields Eye Hospital Special Trustees and Mercer Fund from Fight for Sight (I.L). Portions of this work were performed at Beamline X27A, National Synchrotron Light Source (NSLS), Brookhaven National Laboratory, under a General user grant to JMF. X27A is supported in part by the U.S. Department of Energy (DOE) - Geosciences (DE-FG02-92ER14244 to The University of Chicago - CARS). Use of the NSLS was supported by the DOE, Office of Science, Office of Basic Energy Sciences, under Contract No. DE-AC02-98CH10886. Tissue for this project was provided by the UCL Institute of Ophthalmology and Moorfields Eye Hospital Eye Tissue Repository supported by NIHR funding.

Figures

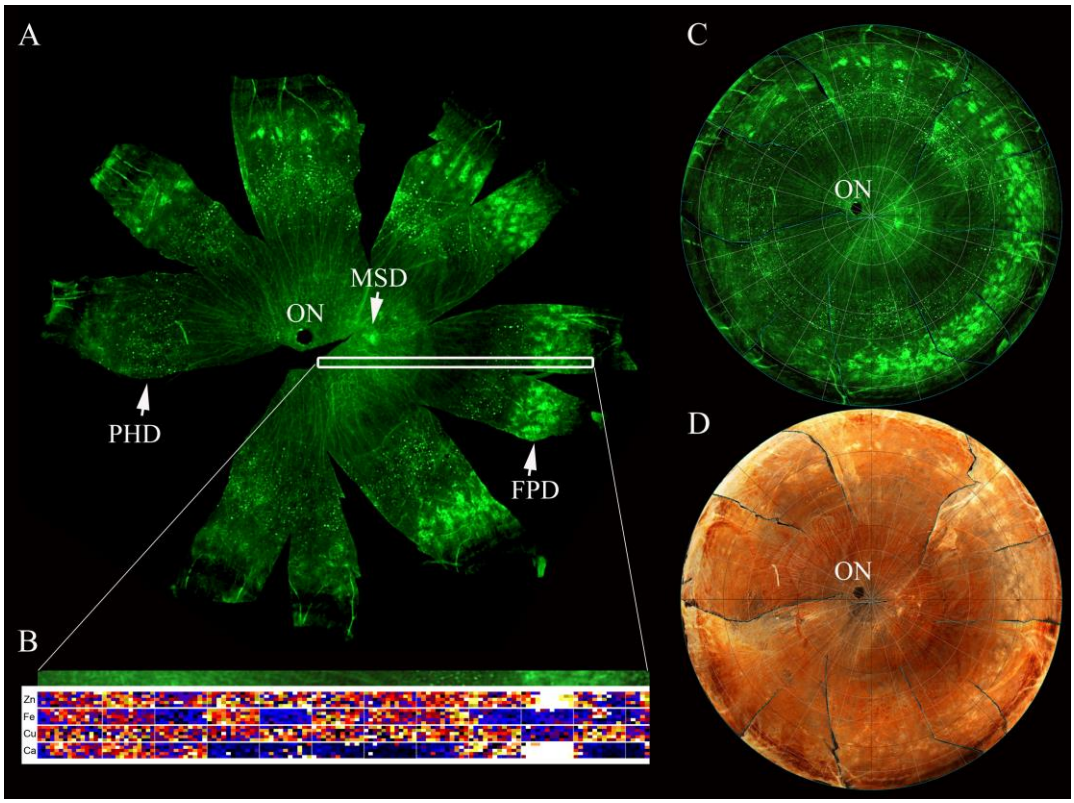

Figure 1. Sub-RPE deposits are widely distributed in a donor eye with early AMD. A) Flat mount whole retina stained with ZinPyr1, showing Zn in macular soft drusen (MSD), peripheral hard drusen (PHD) and far peripheral deposits (FPD). Dissection and relaxing cuts rendered the quasi-spherical retina into a 2D preparation. B) A Bruch's membrane/choroid complex strip (0.4 X 25 mm from *ora serrata* to the macula) showing ZinPy1 fluorescent Zn staining (green strip) and false color images of metal distributions for (from top to bottom) Zn, Fe, Cu and Ca, as determined by μSXRF. The false color images are scaled for the minimum and maximum CPS values for each of the individual metals to allow pixel by pixel comparison. Measurements were taken at every 200 μm with a 10 μm wide beam. C) The algorithm, "Retistruct," reconstructed the retinal flat-mounts on (A) by mapping it into a standard, spherical retinal space. D) The reconstructed view of the bright field image of the flat-mount on (A). ON indicates the position of optic nerve.

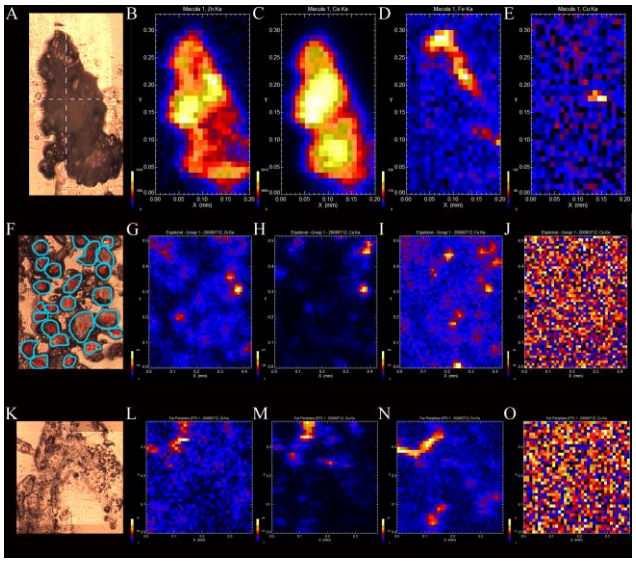

Figure 2. Optical images and false color µSXRF images of the three different sub-RPE deposits. Twenty µm thick sections of the isolated sub-RPE deposits were imaged optically before µSXRF scanning (A, F, K). False color images show Zn (B, G, L), Ca (C, H, M), Fe (D, I, N) and Cu (E, J, O) distribution in MSD, PHD and FPD, respectively. µSXRF images show relative intensities for each metal according to the color bars, where white indicates the maximal CPS values.

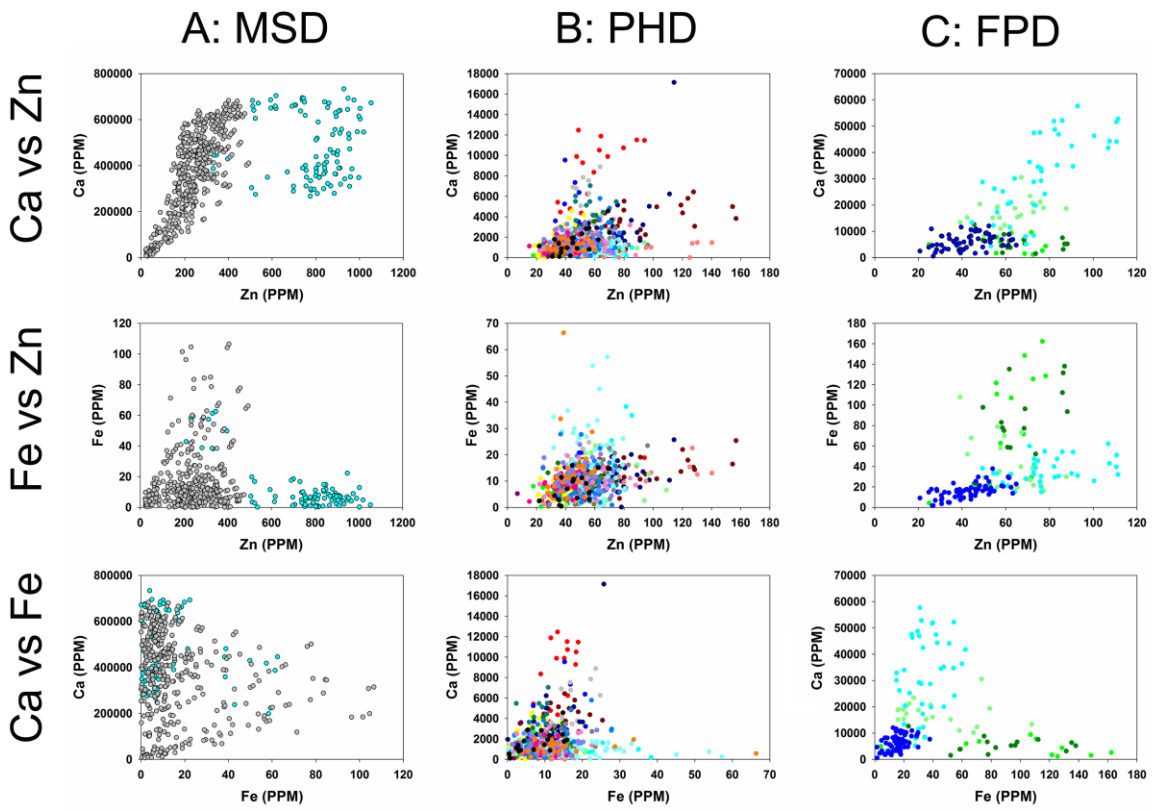

Figure 3. Pixel-by-pixel correlations of metal concentrations (in PPM) of multiple drusen. A) large macular soft drusen (MSD, n=2), B) peripheral hard drusen (PHD n=26), C) far peripheral deposits (FPD, n=5). Pixels from individual druse are color coded for easier comparison.

Table 1. Average metal concentration in sectioned sub-RPE deposits isolated from the three geographic locations. Values are in parts per million (PPM).

	Zn	*Ca*	*Fe*
Macula	380.3 ± 11.4	453 ± 6 x 10^3	11.5 ± 0.8
Periphery	53.7 ± 0.8	1.8 ± 0.1 x 10^3	10.4 ± 0.3
Far Periphery	58.0 ± 1.6	14.0 ± 1.1 x 10^3	37.2 ± 2.8

Table 2. Pixel by pixel correlation between metals in sub-RPE deposits isolated from the three geographic locations. The numbers are R values calculated by linear regression. The numbers of pixels used are indicated in the parenthesis.

	Zn x Ca	*Zn x Fe*	*Fe x Ca*
Macula (n = 752)	0.427	0.159	0.199
Periphery (n = 595)	0.279	0.284	0.178
Far Periphery (n = 149)	0.681	0.422	0.028

References:

1. R. A. Cherny, C. S. Atwood, M. E. Xilinas, D. N. Gray, W. D. Jones, C. A. McLean, K. J. Barnham, I. Volitakis, F. W. Fraser, Y. Kim, X. Huang, L. E. Goldstein, R. D. Moir, J. T. Lim, K. Beyreuther, H. Zheng, R. E. Tanzi, C. L. Masters and A. I. Bush, *Neuron*, 2001, 30, 665-676.
2. A. I. Bush, *Neurobiol Aging*, 2002, 23, 1031-1038.
3. C. W. Levenson, *Nutrition reviews*, 2003, 61, 311-313.
4. C. W. Ritchie, A. I. Bush and C. L. Masters, *Expert Opin Investig Drugs*, 2004, 13, 1585-1592.
5. A. C. Bird, *Eye*, 2003, 17, 457-466.
6. J. W. Crabb, M. Miyagi, X. Gu, K. Shadrach, K. A. West, H. Sakaguchi, M. Kamei, A. Hasan, L. Yan, M. E. Rayborn, R. G. Salomon and J. G. Hollyfield, *Proc Natl Acad Sci U S A*, 2002, 99, 14682-14687.
7. R. J. Ulshafer, C. B. Allen and M. L. Rubin, *Arch Ophthalmol*, 1990, 108, 113-117.
8. C. A. Curcio, M. Johnson, M. Rudolf and J. D. Huang, *The British journal of ophthalmology*, 2011, DOI: 10.1136/bjophthalmol-2011-300344.
9. I. Lengyel, A. Tufail, H. A. Hosaini, P. Luthert, A. C. Bird and G. Jeffery, *Invest Ophthalmol Vis Sci*, 2004, 45, 2886-2892.
10. C. M. Ethen, C. Reilly, X. Feng, T. W. Olsen and D. A. Ferrington, *Invest Ophthalmol Vis Sci*, 2006, 47, 2280-2290.
11. A. S. Neubauer, A. Yu, C. Haritoglou and M. W. Ulbig, *Acta Ophthalmol Scand*, 2005, 83, 758-760.
12. C. W. Ritchie, T. Peto, N. Barzegar-Befroei, A. Csutak, P. Ndhlovu, D. Wilson, B. Corridan, B. Goud, N. Cheesman and I. Lengyel, *Invest. Ophthalmol. Vis. Sci.*, 2011, 52, 6683-.
13. J. M. Seddon, R. Reynolds and B. Rosner, *Investigative ophthalmology & visual science*, 2009, 50, 586-591.
14. S. J. Perkins, A. S. Nealis and R. B. Sim, *Biochemistry*, 1991, 30, 2847-2857.
15. A. M. Blom, L. Kask, B. Ramesh and A. Hillarp, *Archives of biochemistry and biophysics*, 2003, 418, 108-118.
16. R. Nan, I. Farabella, F. F. Schumacher, A. Miller, J. Gor, A. C. Martin, D. T. Jones, I. Lengyel and S. J. Perkins, *J Mol Biol*, 2011, 408, 714-735.
17. R. Nan, J. Gor, I. Lengyel and S. J. Perkins, *J Mol Biol*, 2008.
18. R. Nan, S. Tetchner, E. Rodriguez, P. J. Pao, J. Gor, I. Lengyel and S. J. Perkins, *The Journal of biological chemistry*, 2013, DOI: 10.1074/jbc.M113.476143.
19. S. D. Vogt, C. A. Curcio, L. Wang, C. M. Li, G. McGwin, Jr., N. E. Medeiros, N. J. Philp, J. A. Kimble and R. W. Read, *Experimental eye research*, 2011, 93, 413-423.
20. T. L. van der Schaft, W. C. de Bruijn, C. M. Mooy, D. A. Ketelaars and P. T. de Jong, *Arch Ophthalmol*, 1992, 110, 389-394.
21. J. L. Dunaief, *Investigative ophthalmology & visual science*, 2006, 47, 4660-4664.
22. K. L. Olin, L. S. Morse, C. Murphy, J. Paul-Murphy, S. Line, R. W. Bellhorn, L. M. Hjelmeland and C. L. Keen, *Proc Soc Exp Biol Med*, 1995, 208, 370-377.
23. N. K. Wills, V. M. Sadagopa Ramanujam, N. Kalariya, J. R. Lewis and F. J. G. M. van Kuijk, *Experimental eye research*, 2008, 87, 80-88.

24. I. Lengyel, J. M. Flinn, T. Peto, D. H. Linkous, K. Cano, A. C. Bird, A. Lanzirotti, C. J. Frederickson and F. J. van Kuijk, *Exp Eye Res*, 2007, 84, 772-780.
25. D. C. Sterratt, D. Lyngholm, D. J. Willshaw and I. D. Thompson, *PLoS computational biology*, 2013, 9, e1002921.
26. J. M. Flinn, D. Hunter, D. H. Linkous, A. Lanzirotti, L. N. Smith, J. Brightwell and B. F. Jones, *Physiol Behav*, 2005, 83, 793-803.
27. L. M. Miller, Q. Wang, T. P. Telivala, R. J. Smith, A. Lanzirotti and J. Miklossy, *J Struct Biol*, 2006, 155, 30-37.
28. J. C. Erie, J. A. Good, J. A. Butz and J. S. Pulido, *American journal of ophthalmology*, 2008.
29. R. J. Ulshafer, C. B. Allen, B. Nicolaissen, Jr. and M. L. Rubin, *Investigative ophthalmology & visual science*, 1987, 28, 683-689.
30. D. V. Rao, M. Swapna, R. Cesareo, A. Brunetti, T. Akatsuka, T. Yuasa, T. Takeda and G. E. Gigante, *Journal of X-ray science and technology*, 2010, 18, 327-337.
31. P. Hahn, A. H. Milam and J. L. Dunaief, *Arch Ophthalmol*, 2003, 121, 1099-1105.
32. G. S. Hageman and R. F. Mullins, *Mol Vis*, 1999, 5, 28.
33. D. H. Anderson, G. S. Hageman, R. F. Mullins, M. Neitz, J. Neitz, S. Ozaki, K. T. Preissner and L. V. Johnson, *Invest Ophthalmol Vis Sci*, 1999, 40, 3305-3315.
34. D. H. Anderson, S. Ozaki, M. Nealon, J. Neitz, R. F. Mullins, G. S. Hageman and L. V. Johnson, *American journal of ophthalmology*, 2001, 131, 767-781.
35. G. S. Hageman, P. J. Luthert, N. H. Victor Chong, L. V. Johnson, D. H. Anderson and R. F. Mullins, *Prog Retin Eye Res*, 2001, 20, 705-732.
36. D. H. Anderson, R. F. Mullins, G. S. Hageman and L. V. Johnson, *American journal of ophthalmology*, 2002, 134, 411-431.
37. L. V. Johnson, W. P. Leitner, A. J. Rivest, M. K. Staples, M. J. Radeke and D. H. Anderson, *Proc Natl Acad Sci U S A*, 2002, 99, 11830-11835.
38. L. V. Johnson, W. P. Leitner, M. K. Staples and D. H. Anderson, *Exp Eye Res*, 2001, 73, 887-896.
39. G. Malek, C. M. Li, C. Guidry, N. E. Medeiros and C. A. Curcio, *Am J Pathol*, 2003, 162, 413-425.
40. C. A. Curcio, J. B. Presley, G. Malek, N. E. Medeiros, D. V. Avery and H. S. Kruth, *Exp Eye Res*, 2005, 81, 731-741.
41. T. G. Farkas, V. Sylvester and D. Archer, *American journal of ophthalmology*, 1971, 71, 1196-1205.
42. T. G. Farkas, V. Sylvester, D. Archer and M. Altona, *American journal of ophthalmology*, 1971, 71, 1206-1215.
43. R. Haimovici, D. L. Gantz, S. Rumelt, T. F. Freddo and D. M. Small, *Invest Ophthalmol Vis Sci*, 2001, 42, 1592-1599.
44. R. J. Ulshafer, C. B. Allen, B. Nicolaissen, Jr. and M. L. Rubin, *Invest Ophthalmol Vis Sci*, 1987, 28, 683-689.
45. Z. Molnar, P. Kovacs, I. Laczko, K. Soos, L. Fulop, B. Penke and I. Lengyel, *J Neurochem*, 2004, 89, 1215-1223.
46. S. H. Sarks, J. J. Arnold, M. C. Killingsworth and J. P. Sarks, *The British journal of ophthalmology*, 1999, 83, 358-368.
47. A. Panorgias, R. J. Zawadzki, A. G. Capps, A. A. Hunter, L. S. Morse and J. S. Werner, *Invest Ophthalmol Vis Sci*, 2013, 54, 4372-4384.
48. *Arch Ophthalmol*, 2001, 119, 1417-1436.
49. I. Lengyel and T. Peto, *Expert Rev Ophthalmol*, 2008, 3, 1-4.

Examining the relationship between zinc, calcium, iron and copper in isolated sub-RPE deposits highlighted the diverse role these metals might play in conditions like age-related macular degeneration.